Electric-Field-Induced Transitions of Amphiphilic Layers on Mercury Electrodes

Xiaoping Gao and Henry S. White*

Department of Chemistry, University of Utah, Salt Lake City, Utah 84112

Shaowei Chen and Héctor D. Abruña*

Department of Chemistry, Baker Laboratory, Cornell University, Ithaca, New York 14853

Received April 17, 1995. In Final Form: June 26, 1995[⊗]

There are numerous examples in the literature of amphiphilic molecules which, when adsorbed onto mercury electrodes, undergo electric-field-induced transitions between different molecular conformations. In general, very sharp and reversible voltammetric features associated with these transitions are observed when the electrode potential is scanned in the negative direction, typically over the range of −0.30 to −1.50 V vs SCE, although no redox center is active in these molecular assemblies within this potential range. Using simple electrostatic and thermodynamic arguments, an analytical expression is derived that allows the voltammetric response to be computed in terms of possible molecular conformational changes of the monolayer. The magnitude, shape, and potential of the voltammetric wave are dependent upon molecular parameters (e.g., charge distribution, dimensions, and dielectric properties of the amphiphile), surface coverage, and nonelectrostatic energy contributions. A peak-shaped voltammetric response is shown to be consistent with the redistribution of charged sites within the amphiphilic layer in response to the surface electric field. Numerical results are in qualitative agreement with voltammetric data for dioleoylphosphatidylcholine (DOPC) adsorbed onto mercury electrodes.

Introduction

Amphiphilic molecules, including phospholipid monolayers, have been employed as models for biological membranes in the study of membrane structural transitions and membrane transport.[1-6] Due to the mechanical stability of these layers and their strong resistance to oxidation or reduction, electrochemical techniques have proven quite valuable in the investigation of the electrical properties of these model membranes. Of particular note is the work of Miller and co-workers and Lecompte and co-workers.[7-11] These investigators studied, employing impedance measurements and cyclic voltammetry, the electrochemical behavior of a variety of molecules such as prothrombin at mercury electrodes coated with amphiphilic monolayers and in some cases directly onto the mercury surface itself. Their studies suggested that there was an electrode-potential-induced reorientation of the amphiphilic molecules adsorbed onto mercury.

In more recent investigations, voltammetric techniques have been used to study potential-induced structural changes of phospholipid monolayers that are irreversibly adsorbed onto a Hg electrode.[12-14] For example, Figure 1 presents a steady-state cyclic voltammogram in a 0.20 M KCl solution (at a sweep rate of 100 V/sec) for a Hg electrode coated with an irreversibly-adsorbed monolayer of dioleoylphosphatidylcholine (DOPC). Although no

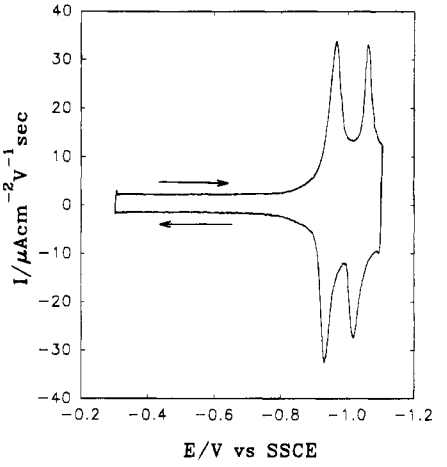

Figure 1. Cyclic voltammetric response of a Hg/DOPC electrode immersed in a N_2-purged 0.20 M KCl solution (pH = 8.2). Scan rate: 100 V/s.

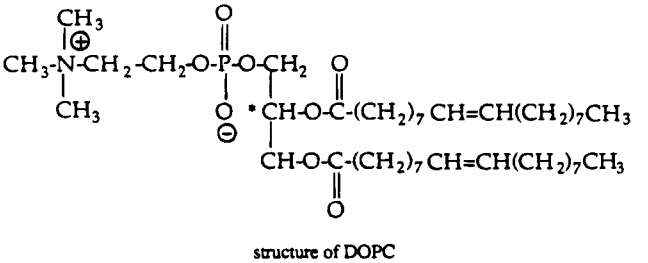

structure of DOPC

[⊗] Abstract published in *Advance ACS Abstracts,* September 1, 1995.

(1) Blank, M.; Miller, I. R. *J. Colloid Interface Sci.* **1967**, *26*, 26.
(2) Phillips, M. C.; Chapman, D. *Biochim. Biophys. Acta* **1968**, *163*, 301.
(3) Sakurai, I.; Kawamura, Y. *Biochim. Biophys. Acta* **1987**, *904*, 405–409.
(4) Seimiya, T.; Miyasaka, H.; Kato, T.; Shirakawa, T.; Ohbu, K.; Iwahashi, M. *Chem. Phys. Lipids* **1987**, *43*, 161–177.
(5) Ibdah, J. A.; Phillips, M. C. *Biochemistry* **1988**, *27*, 7155–7162.
(6) Als-Nielsen, J.; Christensen, F.; Persham, P. S. *Phys. Rev. Lett.* **1982**, *48*, 1107.
(7) Pagano, R. E.; Miller, I. R. *J. Colloid Interface Sci.* **1973**, *45*, 126.
(8) Lecompte, M. F.; Miller, I. R. *Bioelectrochem. Bioeng.* **1988**, *20*, 99.
(9) Lecompte, M. F.; Miller, I. R. *J. Colloid Interface Sci.* **1988**, *123*, 259.
(10) Lecompte, M. F.; Clavillier, J.; Dode, C.; Elion, J.; Miller, I. R. *Bioelectrochem. Bioeng.* **1984**, *13*, 211.
(11) Lecompte, M. F.; Miller, I. R. *Biochemistry* **1980**, *19*, 3439.
(12) Nelson, A.; Benton, A. *J. Electroanal. Chem.* **1986**, *202*, 253–270.
(13) (a) Leermakers, F. A. M.; Nelson, A. *J. Electroanal. Chem.* **1990**, *278*, 53–72. (b) Nelson, A.; Leermakers, F. A. M. *J. Electroanal. Chem.* **1990**, *278*, 73–83.
(14) Chen, S.; Abruña, H. D. *Langmuir* **1994**, *10*, 3343–3349.

0743-7463/95/2411-4554$09.00/0

redox-active center (within the potential range of 0.0 to −1.5 V vs SSCE) is present in these molecular assemblies, two very sharp and reversible waves are observed with peak potentials of −0.90 and −1.1 V, respectively.

The peak-shape voltammetric response shown in Figure 1 is typical of Hg electrodes coated with electroinactive long-chain carboxylic acids,[15] as well as other phospholipids.[12,13] The number of voltammetric waves observed and the electrode potential at which they occur are specific to the chemical nature of the monolayer. However, in all of these cases, the voltammetric response is unquestionably associated with a conformational change within the monolayer, since the molecules that comprise the monolayer are electroinactive within the investigated potential range. We find evidence for such behavior in a variety of publications where amphiphilic *redox-active* molecules adsorbed onto mercury surfaces exhibit additional voltammetric features that are not associated with the redox center in question. Recent examples of these include the work of Schiffrin[16] and co-workers on the electrochemical behavior of ubiquinone (UQ_{10}) adsorbed onto mercury electrodes as well as the work of Tokuda and co-workers[17,18] and Camacho and co-workers[19] on long-chain viologens. In all of these cases, there is a voltammetric feature, not associated with the redox-active center, which can be ascribed to the afore-mentioned potential-induced conformational transitions.

Although there is a qualitative understanding that a transient current will result whenever there is a potential-induced redistribution of surface charge (the above response for adsorbed DOPC (Figure 1) clearly illustrates such behavior), to our knowledge, no theoretical treatment exists which describes the current−voltage response associated with such a process. In the specific case of phospholipid monolayers on Hg electrodes, there have been limited attempts at developing a theoretical framework that allows interpretation of the voltammetric response. Nelson and Leermakers used a statistical model based on Flory−Huggins (F−H) interaction parameters to elucidate the potential-dependent structures of phospholipid monolayers and bilayers on Hg in equilibrium with a solution containing the phospholipid molecule.[13] On the basis of their computations, these authors suggested that the first voltammetric peak in Figure 1 "corresponds to a competition between headgroups and hydrocarbon tails for access to the interface giving rise to an inhomogeneous layer of two phases consisting of a thin bilayer and thin monolayer respectively",[13b] consistent with the reorientation of some fraction of the molecules comprising the film from a tails-down to headgroup-down conformation. This behavior is rationalized by assuming that the affinities of the solvent (H_2O), headgroup, and apolar hydrocarbon tails for the surface are strong functions of the surface hydrophobicity, which is electrode potential dependent and decreases as the electrode potential is moved away from the potential of zero charge (E_{pzc}). Although this description is quite reasonable, unfortunately, no structurally-sensitive experimental measurements (e.g., in situ STM or X-ray diffraction methods) have been made that either support or refute the proposed potential-dependent structures. In addition, values of the F−H interaction parameters for the various potential-dependent surface interactions are not known.[13a]

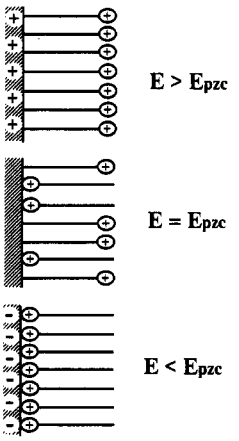

Figure 2. Schematic diagram of the orientation of amphiphilic molecules in response to the electrode potential (relative to the potential of zero charge, E_{PZC}).

More recent theoretical and experimental investigations by Waängnerud and Jönsson have focused of the physical nature of interactions that give rise to adsorption of amphiphiles as bilayers on charged surfaces, including, among several factors, the influence of electrostatic interactions between the surface and charged adsorbed molecules.[20] In this work, electrostatic effects are explicitly treated using the Poisson−Boltzmann equation, yielding testable predictions concerning the nature of adsorbed structures as a function of the surface charge density, electrolyte concentration, and valence of the amphiphile co-ion. A key conclusion of the Wängnerud and Jönsson investigations, supported by in situ ellipsometry, is that the structure of the amphiphile layer is strongly dependent on electrostatic effects, tending to form bilayers at high surface charge densities.

Following the general approach of Wängnerud and Jönsson, a peak-shaped current in the voltammetric response of amphiphilic monolayers irreversibly adsorbed onto Hg can be anticipated by considering the electrostatic forces acting between the charged metal surface and the ionized headgroups on a lipid layer. Consider, for instance, the idealized structures shown in Figure 2 of a lipid monolayer in contact with a metal electrode and immersed in an electrolytic solution. For simplicity, we assume that the molecule has a positively-charged headgroup and that it is possible for the molecule to rapidly change between orientations in which the headgroup is at the metal/lipid interface or at the lipid/solution interface. When the potential of the electrode is sufficiently positive of the potential of zero charge ($E > E_{PZC}$), such that the electrode surface has a net positive charge density, there will be a tendency for the molecules to orient such that the headgroups are located at the lipid/solution interface, thereby reducing the electrostatic repulsion between the surface and lipid layer. Conversely, when the electrode potential is negative of the E_{PZC}, the electrostatic attraction between the negatively charged electrode and positively charged molecule will tend to orient the molecule with the headgroup at the metal/lipid layer interface.

The reorientation of the lipid layer results in the movement of a net charge through the electric field that exists across the lipid layer. For the phospholipid corresponding to the data in Figure 1, the effective distance that charge is moved is on the order of the length of the molecule (~25 Å). This displacement of charge will alter

(15) Orzechowska, M.; Matysik, J. *J. Electroanal. Chem.* **1979**, *103*, 251−259.
(16) Gordillo, G. J.; Schiffrin, D. J. *J. Chem. Soc., Faraday Trans.* **1994**, *90*, 1913.
(17) Kitamura, F.; Ohsaka, T.; Tokuuda, K. *J. Electroanal. Chem.* **1994**, *368*, 281.
(18) Kitamura, F.; Ohsaka, T.; Tokuuda, K. *Chem. Lett.* **1991**, 375.
(19) Sánchez Maestre, M.; Rodríguez-Amaro, R.; Muñoz, E.; Ruiz, J. J.; Camacho, L. *J. Electroanal. Chem.* **1993**, *359*, 325.
(20) Wängnerud, B.; Jönsson, B. *Langmuir* **1994**, *10*, 3268−78.

the preexisting electric field, resulting in a measurable flow of current at the electrode surface. This current is associated only with charging of the interface required to minimize the electrical energy (and, thus, overall free energy) and does not involve any redox chemistry.

Although the structures and conformational transition depicted in Figure 2 are highly speculative, and perhaps unrealistic based on energetic considerations, we will employ this model for the sole purpose of demonstrating a general method of computing the voltammetric current resulting from a potential-dependent conformational change. As will be discussed in a later section, the methodology described here may be readily adapted to other structures (including amphiphilic bilayers), as well as other potential-dependent interactions (such as solvent dipole reorientation), allowing the voltammetric response to be computed for structures that are deduced from future experimental measurements.

As noted above, no theoretical treatment exists which allows prediction or interpretation of the voltammetric response associated with such a conformational transition. Consequently, prior voltammetric investigations of amphiphilic monolayers have not provided quantitative information concerning the structural features of the monolayer nor the dynamics of potential-dependent conformational changes. On the other hand, voltammetric techniques for investigating electroactive monolayers, e.g., self-assembled monolayers with pendant redox groups,[21] are well-established and provide a quantitative means of measuring kinetic and thermodynamic parameters associated with electron transfer, the number density of electroactive molecules within the film, and the chemical stability of the monolayer in different oxidation states.[22] In addition, recent theoretical and experimental investigations have shown that the voltammetric responses of an irreversibly adsorbed electroactive monolayer[23] and monolayers containing acid/base groups[24] are very sensitive to structural details of the adsorbed molecule (e.g., chain length, valence) as well as to parameters that influence the interfacial potential distribution (e.g., ionic strength of the contacting solution). These latter developments suggest that similar structural information concerning amphiphilic films might be obtained by electrochemical measurements.

On the basis of success of voltammetric techniques in characterizing electroactive films, our laboratories have recently initiated an investigation of the factors that determine the peak-shaped voltammetric response of nonelectroactive monolayers, with the prospect of applying the results to amphiphilic monolayers. This report describes the first approach based on integrating electrostatic and thermodynamic arguments describing the film conformations, with the relevant equations describing the perturbation and response functions of the voltammetric experiment. Because of the mathematical complexities that underlie an accurate description of the film structure, especially at the microscopic level, as well as those associated with the electroanalytical method, a number of simplifications have been made in order to yield a tractable problem. Nevertheless, the results represent the first quantitative model of the voltammetric response of an electroinactive amphiphilic monolayer and are conceptually useful in understanding how the peak-shaped current response is related to the structure of the monolayer and its electrostatic environment.

Experimental Section

Dioleoylphosphatidylcholine (DOPC, approximately 99%) was used as received from Fluka. Solutions of 0.20 mg of DOPC/mL of chloroform were prepared just prior to use. Electrolyte solutions were prepared with ultrapure (at least 99.99+%) salts (Aldrich), which were dissolved (0.20 M) in water which was purified with a Milli-Q system and buffered with high-purity phosphate salts or hydrochloric acid (all from Aldrich) depending on the desired pH.

Electrochemical experiments were carried out with an EG&G PARC 173 potentiastat and 175 Universal Programmer. Data were collected on a Nicolet 4094 digital oscilloscope and transferred to a personal computer for analysis.

A sodium-saturated calomel electrode (SSCE) was used as the reference electrode, and a large-area platinum coil was used as the counter electrode. The working electrode was a Kemula-type (micrometer driven) hanging mercury drop electrode (HMDE), which was filled with high-purity mercury (electronic grade, 99.9998% from Johnson Matthey). A two-compartment cell without frits was employed in all experiments. The cell had standard joints for all electrodes and for degassing.

The detailed experimental procedures have been described previously.[12,14] Figure 1 shows the typical voltammetric response (at 100 V/s) for a DOPC monolayer adsorbed on a Hg electrode surface in a 0.20 M KCl solution (pH = 8.2). Two very sharp and reversible waves centered at about −0.9 and −1.0 V, respectively, are clearly evident. A qualitatively similar response was observed over the pH range from 0.7 to 9.2. However, the potentials at which these two waves appeared as well as their sharpness were dependent on pH and on the nature of the electrolyte. Such effects and trends have been reported earlier.[12]

Results and Discussion

An expression that describes the voltammetric behavior of electroinactive lipid layers is developed in the following order. In subsection I, an electrostatic model of the interface that incorporates the essential features of the assembled phospholipid layer is introduced. General analytic expressions are presented which relate the applied electrode potential in a voltammetric experiment to the orientation of the lipid molecules on the surface and to other electrostatic parameters that influence the overall interfacial charge and potential distributions (e.g., electrolyte concentration and dielectric constant). In subsection II, an expression for the free energy of the lipid molecules is introduced which allows the configuration of the molecular layer to be computed as a function of the interfacial potential distribution. The electrostatic and thermodynamic expressions are combined in subsection III to obtain the general current−potential response expected in a voltammetric experiment. In subsection IV, theoretical voltammograms are presented for a variety of system parameters (e.g., surface coverage, molecular dimensions, degree of lipid ionization), and in subsection V, the results are compared to experimental data.

The general strategy used in developing a model for the voltammetric response of these lipid monolayers is similar to that reported earlier for analyzing the behavior of the monolayers containing redox or acid/base functionalities.[23,24]

I. Interfacial Potential and Charge Distribution. Figure 3 shows the electrostatic model used to compute the interfacial potential distribution. The model consists of a tightly-packed lipid monolayer assembled on a planar metal electrode of area A (cm^2) and immersed in an electrolyte solution that contains a symmetric z:z electrolyte. The solution is assigned a dielectric constant, ϵ_s.

(21) (a) Chidsey, C. E. D. *Science* **1991**, *7*, 919. (b) Findklea, H. O.; Hanshew, D. D. *J. Am. Chem. Soc.* **1992**, *64*, 2398. (c) Rowe, G. R.; Creager, S. E. *Langmuir* **1991**, *7*, 2307.

(22) Bard, A. J.; Faulkner, L. R. *Electroanalytical Methods*; Wiley: New York, 1980.

(23) (a) Smith, C. P.; White, H. S. *Anal. Chem.* **1992**, *64*, 2398−2405. (b) Fawcett, W. R. *J. Electroanal. Chem.* **1994**, *378*, 117−24.

(24) (a) Smith, C. P.; White, H. S. *Langmuir* **1993**, *9*, 1−3. (b) Fawcett, W. R.; Fedurco, M.; Kovacova, T. *Langmuir* **1994**, *10*, 2403−10.

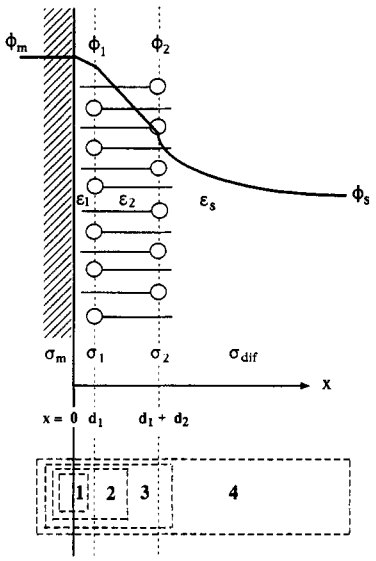

Figure 3. Model system used to calculate the charge distribution and electric field in the amphiphilic monolayer.

The lipid monolayer assembly can be modeled in several ways that strongly depend on the assumed molecular conformation and the degree of dissociation of headgroup functionalities. For instance, at moderate and high pH values, DOPC exists as a zwitterionic species (see structure), whereas at low pH (pH < 2), the phosphate group is protonated, leaving the headgroup with a net positive charge. As mentioned earlier, the voltammetric response is slightly dependent on pH, but two reversible voltammetric peaks, similar to the response shown in Figure 1, are observed at all pH's.

The model we assume, and schematically shown in Figure 3, is that of an electrode surface covered by two dielectric films of thicknesses d_1 and d_2 with dielectric constants ϵ_1 and ϵ_2, respectively. Distance d_1 is defined as the distance between the surface and the positive site when the lipid headgroup is located at the electrode/lipid interface. It is difficult to obtain a precise value for d_1 without detailed structural information concerning the orientation of the headgroup at the surface. However, based on the molecular structure shown earlier, it is likely that this distance has a value between 2 and 3 Å. The thickness of the dielectric layer d_2 is defined as the length of the molecule minus the length d_1. A transition between the inward (headgroups-down) and outward (tails-down) orientations will result in a displacement of the positive charge on the molecule by a distance of $d_2 - d_1$.

The surface coverages of lipid molecules oriented with their polar headgroups at the electrode/lipid and lipid/solution interfaces are designated as Γ_1 and Γ_2, respectively. Since the molecules are irreversibly adsorbed, the total surface coverage, Γ_T, is defined as $\Gamma_T = \Gamma_1 + \Gamma_2$.

To simplify the resulting expressions, we will assume that each lipid molecule possesses a single net positive charge, z_{mol}. For the low-pH DOPC structure, we anticipate $z_{mol} \sim +1$. From electrostatic considerations, at high pH, the zwitterionic form of DOPC would be expected to behave equivalently to a positively charged species, with z_{mol} less than +1. This conclusion is based on the dipole nature of the zwitterion, in which the positively charged choline group undergoes a slightly larger spatial translation than the negatively charged phosphate group (~4–6 Å based on the molecular dimensions discussed above) during the assumed conformational transition. Thus, the image charge (voltammetric current) induced in the metal during the conformational transition of the zwitterion will be equivalent to that generated by the transition of a molecule containing a small positive charge. However, these general arguments could be somewhat compromised by the fact that ion association between the amphiphilic molecules and dissolved counterions may be significant, albeit unknown.[25] As detailed below, this latter limitation prevents an independent measurement of z_{mol} and Γ_T using voltammetric data. However, the charge surface density, $z_{mol}\Gamma_T$, involved in the conformational transition is directly measurable.

Assuming that there is no charge in the film except that associated with the charged headgroups ($0 \le z_{mol} \le +1$), the potential will decay linearly from ϕ_m to ϕ_1 and from ϕ_1 to ϕ_2. In the solution phase ($x > d_1 + d_2$), the potential is assumed to be governed by the Gouy–Chapman model and decays to ϕ_s in the bulk solution:

$$\tanh(ze(\phi(x) - \phi_s)/2kT) = \tanh(ze(\phi_2 - \phi_s)/2kT)\exp(-\kappa(x - (d_1 + d_2)))$$

where $\phi(x)$ is the potential (V) in the solution at position x, κ is the inverse Debye length (m^{-1}) given by $\kappa = (z^2e^2 2n^\circ/\epsilon_0\epsilon_s kT)^{1/2}$, e is the charge of an electron (C), n° is the number concentration of the ions in the electrolyte (cm^{-3}), ϵ_0 is the permittivity of free space ($C^2\ N^{-1}\ cm^{-2}$), and k is Boltzmann's constant ($J\ K^{-1}$).

In addition to the above assumptions, we also assume that charges on the metal surface (at $x = 0$) and on the headgroups (at d_1 and $d_1 + d_2$) are delocalized (i.e., discreteness of charge is ignored). Inclusion of the finite size of ions in the description of the electrochemical behavior of redox and acid/base functionalized monolayers on electrodes has been recently discussed by Fawcett and co-workers.[23b,24b] As will be shown below, the potential distribution of the system we are considering is dominated by the capacitance of the dielectric region corresponding to the hydrocarbon tail (i.e., the region defined by $d_2 - d_1$). Thus, the approximation of delocalized charges outside of this region (i.e., at the metal and solution interfaces) appears reasonable.

The electrostatic force exerted on the lipid molecules at any applied electrode potential can be obtained by considering the relationship between the potential distribution and the charge densities on the metal, at positions d_1 and $d_1 + d_2$ and in the electrolyte solution. Since the electrode surface area is generally of the order of cm^2, and the interfacial distances d_1, d_2, and κ^{-1} are of the order of nm, it is only necessary to consider the potential distribution normal to the surface. With attention drawn to Figure 3, the electric field ($E = -dV/dx$) within each region of the interface is given by

$$E = 0\ (\because \epsilon_m = \infty) \qquad x < 0$$

$$E = (\phi_m - \phi_1)/d_1 \qquad 0 < x < d_1$$

$$E = (\phi_1 - \phi_2)/d_2 \qquad d_1 < x < d_1 + d_2$$

$$E = \frac{\kappa 2kT}{ze}\sinh\left[\frac{ze(\phi_2(x) - \phi_s)}{2kT}\right] \qquad x > d_1 + d_2$$

$$E = 0 \qquad x \to \infty \tag{1}$$

The electric fields and the charge densities associated with the metal, lipid layer, and solution are related through Gauss' law. The Gaussian boxes shown in Figure 3 enclose the charges of interest. For the assumed planar

(25) Meijer, L. A.; Leermakers, F. A. M.; Nelson, A. *Langmuir* **1994**, *10*, 1199–1206.

geometry, the electric field passes only through the faces of the boxes, each of surface area S. Thus,

$$Q_i = \epsilon_0\epsilon_i \int_S \vec{E}_i \, d\vec{S}_i = \epsilon_0\epsilon_i E_i S \qquad (2)$$

Combining eqs 1 and 2 and applying the result to the four boxes shown in Figure 3 yield the following system of equations relating the charge densities ($\sigma_i = Q_i/S$) and interfacial potentials:

$$\sigma_m = \epsilon_0\epsilon_1(\phi_m - \phi_1)/d_1 \quad \text{box 1} \qquad (3a)$$

$$\sigma_m + \sigma_1 = \epsilon_0\epsilon_2(\phi_1 - \phi_2)/d_2 \quad \text{box 2} \qquad (3b)$$

$$\sigma_{dif} = -\epsilon_0\epsilon_s\kappa\left(\frac{2kT}{ze}\right)\sinh\left(\frac{ze(\phi_2 - \phi_s)}{2kT}\right) \quad \text{box 3} \qquad (3c)$$

$$\sigma_m + \sigma_1 + \sigma_2 + \sigma_{dif} = 0 \quad \text{box 4} \qquad (3d)$$

where the definitions of charge densities (C cm^{-2}) on the electrode surface (σ_m), at the planes of the lipid headgroups (σ_1, σ_2), and in the solution (the diffuse layer) (σ_{dif}) are given by

$$\sigma_i = \sigma_m \quad x = 0$$

$$\sigma_i = \sigma_1 \quad x = d$$

$$\sigma_i = \sigma_2 \quad x = d_1 + d_2$$

$$\sigma_i = \sigma_{dif} \quad d_1 + d_2 < x < \infty \qquad (4)$$

As has been indicated earlier, the lipid layer is electrochemically inactive and irreversibly adsorbed over the potential range of interest. Thus, the total charge per unit area in the film is constant; i.e.,

$$\sigma_1 + \sigma_2 = z_{mol}F\Gamma_T \qquad (5)$$

II. Relationship between Local Potential and Molecular Orientation. In order to calculate the voltammetric response corresponding to the field-induced transition, it is necessary to establish a relationship between the two assumed molecular orientations and the electrode potential. As previously noted, the molecular orientation is anticipated to be a function of the applied potential if the electrostatic forces between the charges on the metal surface and on the lipid molecule are sufficiently large to flip the molecules between the inward and outward-directed configurations, Figure 2. The fact that a reversible voltammetric response, Figure 1, is observed even at relatively high scan rates (e.g., 100 V/s) suggests that this process is facile on the time scale of the electrochemical experiment and that the equilibrium structure is determined, to a significant extent, by the interfacial potential distribution.

To account for the influence of the electrostatic potential on the molecular orientation, we assume that the electrochemical potential of the lipid molecules is given by

$$\bar{\mu}_j = \mu_j^\circ + RT \ln a_j + z_{mol}F\phi_j \qquad (6)$$

where F, R, and T are Faraday's constant (C mol^{-1}), the molar gas constant (J mol^{-1} K^{-1}), and the absolute temperature (K), respectively. The subscript j refers to the two possible molecular orientations (inward ($j = 1$) and outward ($j = 2$)) of the molecules adsorbed on the electrode surface. The constants μ_1° and μ_2° indicate nonelectrostatic energy terms corresponding to hydrophobic/hydrophilic interactions, dispersion and solvation forces, and steric effects associated with the amphiphilic layer in the inward and outward orientations, respectively. We treat these terms as being independent of the electrode potential, since the predominant potential-dependent interactions with the electrode surface are likely to involve electrostatic forces between the surface charge and the fixed charge on the headgroup. The reader is referred to the thorough discussion of Wängnerud and Jönsson[20] for a detailed physical description and estimation of the nonelectrostatic work terms.

At equilibrium, $\bar{\mu}_1 = \bar{\mu}_2$. Approximating the activities a_1 and a_2 by their respective surface concentrations, Γ_1 and Γ_2, yields the relationship between the electrostatic potential distribution in the film and the orientation of the charged sites:

$$\phi_1 - \phi_2 = -\frac{\mu_1^\circ - \mu_2^\circ}{z_{mol}F} - \frac{RT}{z_{mol}}\ln\frac{\Gamma_1}{\Gamma_2} \qquad (7)$$

Equation 7 is simplified by defining $f = \Gamma_1/\Gamma_T$ and the potential $E^\circ = -(\mu_1^\circ - \mu_2^\circ)/z_{mol}F$, yielding

$$\phi_1 - \phi_2 = E^\circ - \frac{RT}{z_{mol}F}\ln\left(\frac{f}{1-f}\right) \qquad (8)$$

It is clear that the potential E° represents the difference in the standard-state chemical potentials of the assumed molecular conformations, and in this sense, its use is similar to that employed in defining the standard redox potentials of electron-transfer reactions (where μ_1° and μ_2° represent the standard-state chemical potentials of the reduced and oxidized partners of the redox couple). As detailed in a later section, the peak position of the voltammetric wave corresponding to a conformational transition is primarily determined by the value of E° (vs a yet specified reference potential). Experimental variables that affect the electrostatic potential distribution (i.e., dielectric constant, ion concentration) have a smaller but significant effect on the potential at which the structural transition is observed.

Admittedly, the model that we have assumed for the potential-dependent conformational transition may not be necessarily correct and clearly does not include all of the features necessary to describe the actual amphiphilic layer. However, although it is beyond the scope of this preliminary treatment, both the electrostatic and thermodynamic treatments outlined above may be readily modified when considering different structures and potential-dependent interactions. For instance, the Gaussian box approach used above can be readily extended to include a true zwitterionic structure, requiring only the addition of an additional charged layer in the model scheme (Figure 3) and one additional application of Gauss' law (eq 2). In analogous fashion, the electrostatic model can be extended to bilayer structures and ion association, and finite ion size effects may be included, as was recently done by Fawcett for self-assembled redox and acid/base monolayers. Similarly, the thermodynamic expressions we assume are highly idealized in many respects. A key deficiency is the implicit assumption that the energetics of reorientation of any molecule within the film are independent of the state of orientation of the neighboring molecules; i.e., the probability of a molecule being in an up or down configuration is independent of the orientational state of the neighboring molecules. Lateral electrostatic interactions within the film will likely make the random approximation improbable. This problem can be treated by methods similar to those developed by Levine *et al.*[26] for accounting for lateral dipole–dipole interactions within adsorbed solvent layers or in a more heuristic

fashion by employing an adjustable interaction parameter in eq 6 (equivalent to employing a Frumkin-type isotherm).

III. Voltammetric Response. If the electrode potential is scanned at a constant rate ν (V/s), the voltammetric response of an electrode coated with an electrochemically-inert film is due only to the capacitive charging current:

$$i = \nu A C_T \tag{9}$$

In eq 9, C_T is the total capacitance (F cm^{-2}) of the interface, which can be evaluated using the formal definition $C_T = \partial\sigma_m/\partial E = \partial\sigma_m/\partial\phi_m$. In deriving an expression for C_T, it is convenient to define the following interfacial capacitances:

$$C_1 = \epsilon_0\epsilon_1/d_1 \tag{10a}$$

$$C_2 = \epsilon_0\epsilon_2/d_2 \tag{10b}$$

$$C_{dif} = \epsilon_0\epsilon_s\kappa \cosh[ze(\phi_2 - \phi_S)/2kT] \tag{10c}$$

C_1 and C_2 represent the potential-independent capacitances of the film, and C_{dif} is the potential-dependent diffuse layer capacitance.

The total interfacial potential drop ($\phi_m - \phi_s$) is equal to the sum of the individual contributions across the interface:

$$\phi_m - \phi_s = (\phi_m - \phi_1) + (\phi_1 - \phi_2) + (\phi_2 - \phi_s) \tag{11}$$

Substituting eqs 3 and 10 into eq 11 yields

$$\phi_m = C_1^{-1}\sigma_m + C_2^{-1}(\sigma_m + \sigma_1) + \phi_2 \tag{12}$$

Differentiating eq 12 with respect to σ_m yields the potential-dependent interfacial capacitance of the system:

$$C_T^{-1} = C_1^{-1} + C_2^{-1}\left(1 + \frac{\partial\sigma_1}{\partial\sigma_m}\right) + \frac{\partial\phi_2}{\partial\sigma_m} \tag{13}$$

Expressing the quantity $\partial\phi_2/\partial\sigma_m$ as $(\partial\phi_2/\partial\sigma_{dif})/(\partial\sigma_m/\partial\sigma_{dif})$ and noting that $\partial\sigma_m/\partial\sigma_{dif} = -1$ (from eqs 3d and 5) and $\partial\phi_2/\partial\sigma_{dif} = -C_{dif}^{-1}$ (from eqs 3c and 10c) yield

$$C_T^{-1} = C_1^{-1} + C_2^{-1}\left(1 + \frac{\partial\sigma_1}{\partial\sigma_m}\right) + C_{dif}^{-1} \tag{14}$$

An explicit expression for $\partial\sigma_1/\partial\sigma_m$ in terms of f is derived from the definition of σ_m. Substituting eq 8 into eq 3b (along with the definition $\sigma_1 = z_{mol}fF\Gamma_T$) yields

$$\sigma_m = \frac{\epsilon_0\epsilon_2}{d_2}\left[E^\circ + \frac{RT}{z_{mol}F}\ln\left(\frac{1-f}{f}\right)\right] - z_{mol}fF\Gamma_T \tag{15}$$

which is differentiated with respect to σ_1:

$$\frac{\partial\sigma_1}{\partial\sigma_m} = \frac{\partial\sigma_1/\partial f}{\partial\sigma_m/\partial f} = -\left[\frac{\epsilon_0\epsilon_2}{d_2}\frac{RT}{z_{mol}^2F^2\Gamma_T}\frac{1}{f(1-f)} + 1\right]^{-1} \tag{16}$$

Since $0 \le f \le 1$, the bracketed expression of eq 16 is always positive, and therefore, $\partial\sigma_1/\partial\sigma_m$ must always be negative. Physically, this relationship indicates that an increase in the positive charge on the electrode must result in a decrease in the positive charge at $x = d_1$ and, conversely, that an increase in the negative surface charge will result in an increase in the positive charge at d_1.

(26) Levine, S.; Bell, G. M.; Smith, A. L. *J. Phys. Chem.* **1969**, *73*, 3534.

Combining eqs 9, 14, and 16 yields the voltammetric current for the amphiphilic monolayer-coated electrode in terms of f:

$$i = \nu A\left\{C_1^{-1} + C_2^{-1}\left(1 - \left[\frac{\epsilon_0\epsilon_2}{d_2}\frac{RT}{z_{mol}^2F^2\Gamma_T}\frac{1}{f(1-f)} + 1\right]^{-1}\right) + C_{dif}^{-1}\right\}^{-1} \tag{17}$$

Before proceeding to the numerical calculations, it is instructive to note that the voltammetric current will be dominated by the smallest individual capacitance of the interface. Consider, for example, a lipid layer with $d_1 \approx 4$ Å, $d_2 = 30$ Å, and $\epsilon_1 = \epsilon_2 = 4$, immersed in an aqueous solution containing 0.10 M of a 1:1 supporting electrolyte ($\epsilon_s = 78$ and $\kappa^{-1} \sim 10$ Å). From eq 10, $C_1 \approx 10$ μF/cm^2, $C_2 \approx 1.5$ μF/cm^2, and $C_{dif}^{min} \approx 90$ μF/cm^2 (where C_{dif}^{min} is the minimum diffuse layer capacitance evaluated at $\phi_2 = \phi_s$). Thus, the voltammetric current will be dominated by the capacitance associated with the hydrocarbon tail, C_2, and the variation of $C_2^{-1}(1 + \partial\sigma_1/\partial\sigma_m)$, eq 14, with the electrode potential will largely determine the shape of the voltammetric response. A maximum in the voltammetric curve is expected, since as the film structure changes from a fully inward orientation ($f = 1$) to a fully outward orientation ($f = 0$), the quantity $\partial\sigma_1/\partial\sigma_m$ changes from 0 to a negative value (see eq 16) and $C_2^{-1}(1 + \partial\sigma_1/\partial\sigma_m)$ decreases.

As the film becomes either completely headgroup directed inward or outward relative to the electrode surface (i.e., as $f \to 1$ or $f \to 0$), $\partial\sigma_1/\partial\sigma_m \to 0$ and eq 14 reduces to the expression for the total capacitance of a film in which no conformational changes are present:

$$C_T^{-1} = C_1^{-1} + C_2^{-1} + C_{dif}^{-1} \tag{18}$$

IV. Computational Results. The voltammetric response is obtained by calculating the current and applied potential as a function of f. The current, i, is obtained directly from eq 17. An explicit expression for the electrode potential, E ($=\phi_m - \phi_s$), is readily obtained by solving eq 3c for ϕ_2 (using the identity $\sinh^{-1}[u] = \ln[u + (u^2 + 1)^{0.5}]$) and substituting the result into eq 12, along with the definitions $\sigma_1 = z_{mol}fF\Gamma_T$, $\sigma_1 + \sigma_2 = z_{mol}F\Gamma_T$, and $\sigma_{dif} = -(\sigma_m + \sigma_1 + \sigma_2)$ (eq 3d). The result is given in eq 19, where σ_m (eq 15) is computed for each specified value of f.

$$E = C_1^{-1}\sigma_m + C_2^{-1}(\sigma_m + z_{mol}fF\Gamma_T) + (2kT/ze)\ln\left\{\frac{ze(\sigma_m + z_{mol}F\Gamma_T)}{2\epsilon_0\epsilon_s\kappa kT} + \left[1 + \left(\frac{ze(\sigma_m + z_{mol}F\Gamma_T)}{2\epsilon_0\epsilon_s\kappa kT}\right)^2\right]^{0.5}\right\} \tag{19}$$

Equations 17 and 19 completely describe the voltammetric response in terms of the properties of the lipid layer (surface coverage, charge, molecular dimensions, and dielectric), the solution phase (electrolyte concentration, charge, and solution dielectric), and temperature. The following independent parameters are input into each calculation: E°, $\epsilon_0\epsilon_1/d_1$ ($=C_1$), $\epsilon_0\epsilon_2/d_2$ ($=C_2$), $z_{mol}\Gamma_T$, κ^{-1}, z, T, ν, and A. All calculations presented are computed for $T = 300$ K and $z = 1$. Unless stated otherwise, E° is taken to be equal to E_{PZC} (i.e., $E^\circ = 0$). Anodic and cathodic currents are mirror images of each other, since the lipid layer is assumed to be in equilibrium with the electrode potential at all times. Only the cathodic current will be presented in the figures. Electrode potentials, E, are referenced to the potential of zero charge, E_{pzc}, of the bare

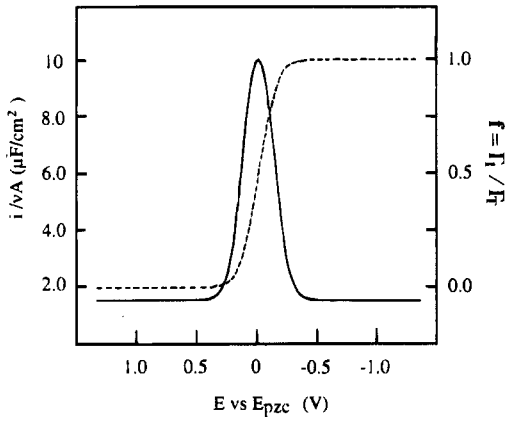

Figure 4. Voltammetric response (solid line) of a Hg electrode coated with a amphiphilic monolayer, calculated from eqs 17 and 19 using the following parameters: $E^\circ = 0$, $z_{mol} = 0.5$, $\Gamma_T = 6 \times 10^{-11}$ mol/cm^2, $\epsilon_1/d_1 = 5$ Å^{-1}, $\epsilon_2/d_2 = 0.182$ Å^{-1}, $C_{elec} = 0.10$ M, $z = 1$, $\epsilon_3 = 78$, and $T = 300$ K. Fraction of lipid molecules ($f = \Gamma_1/\Gamma_T$) oriented with charged headgroup toward the electrode surface (dashed line).

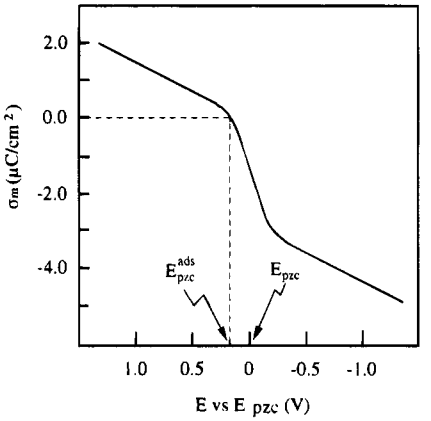

Figure 5. Relationship between charge density on the metal (σ_m) and electrode potential (E). The dashed line indicates the shift in the E_{PZC} due to the adsorbed monolayer (relative to a bare electrode). System parameters used in calculation are the same as in Figure 4.

electrode (i.e., in the absence of the adsorbate; as shown below, the adsorption of the lipid layer induces a significant shift in the E_{pzc}). Voltammetric currents are normalized to the scan rate and electrode area ($i/\nu A$).

Figure 4 shows a voltammogram calculated using the following parameters: $z_{mol} = 0.5$, $\Gamma_T = 6 \times 10^{-11}$ mol/cm^2, $\epsilon_1/d_1 = 10/2$ Å^{-1}, $\epsilon_2/d_2 = 6/33$ Å^{-1}, $\epsilon_s = 78$, and $\kappa^{-1} = 9.6$ Å (corresponding to a 0.10 M aqueous solution of a 1:1 electrolyte). These values are chosen to illustrate the general electrochemical behavior of a lipid-monolayer-coated Hg electrode. In later sections, the effects of varying each parameter will be examined in detail.

Qualitatively, the shape of the theoretical voltammogram is in good agreement with the first voltammetric wave observed for a Hg/DOPC electrode in a pH 8.2, 0.20 M KCl solution (Figure 1). (As previously noted, the simplified model we have assumed does not account for the formation of the final bilayer structure, proposed as the origin of the second cathodic wave;[13] thus, hereafter, all comparisons between experiment and theory refer only to the first wave.) A peak-shaped voltammetric response is observed, centered slightly negative of E_{PZC}. As shown below, the potential corresponding to the current maximum and the wave shape are dependent on E°, z_{mol}, Γ_T, ϵ_s, κ^{-1}, and the capacitances of the lipid monolayer (ϵ_1/d_1 and ϵ_2/d_2).

The shape of the voltammetric wave, Figure 4, is similar to that expected for an electrode coated with an irreversibly adsorbed monolayer of an *electroactive* species. It is thus especially interesting that the theoretical voltammogram is entirely due to capacitive charging of the interface and does not involve the transfer of electrons. A physical explanation of the voltammetric response is illustrated in Figure 4, which shows the fraction of molecules with polar headgroups oriented toward the interface, $f = \Gamma_1/\Gamma_T$ (dashed line), plotted as a function of the electrode potential. At positive potentials, i.e., $E > E_{PZC}$, f is essentially equal to 0, indicating that all of the lipid molecules in the film are oriented with their headgroups oriented away from the interface. Under these conditions, the capacitance of the electrode is essentially constant, since the total electrode capacitance, $C_T^{-1} = C_1^{-1} + C_2^{-1} + C_{dif}^{-1}$, eq 18, is dominated by the smallest individual capacitance, which corresponds to the potential-independent C_2. Consequently, a constant "background or baseline" charging current is observed at values of E sufficiently positive of E_{PZC}. The capacitance calculated from this constant current is ~2 μF/cm^2, in reasonable agreement with the experimental value obtained from Figure 1 (2.5 μF/cm^2). At potentials slightly positive of E_{PZC}, the lipid molecules that comprise the film begin to flip from an outward orientation to an inward orientation, due to the decrease in the electrostatic repulsion between the positive headgroups and the positively charged surface. The quantity f increases monotonically as the potential is scanned negative of E_{PZC}, and at sufficiently negative potentials, f approaches 1 as the electrostatic attraction between the headgroups and the negative surface causes a complete inward-directed orientation of the molecular film.

Further insight into the origin of the voltammetric current is obtained by examining the charge density on the electrode surface, σ_m, as a function of the applied potential, E. Figure 5 shows σ_m vs E (computed using eqs 15 and 19) for the same set of parameters used in computing the voltammetric response in Figure 4. At potentials sufficiently positive or negative of the E_{PZC}, the slope of σ_m vs E is constant, indicating, as before, that the electrode capacitance ($C_T = \partial\sigma_m/\partial E$) is dominated by the potential-independent lipid-layer capacitance, C_2. Near E_{pzc}, σ_m changes rapidly in response to the reorientation of adsorbed molecules. The peak-shaped voltammogram of Figure 4 is the result of the flow of electrons to the electrode surface (but not across the interface) in response to the field-induced movement of the positive charge on the lipid molecule toward the surface.

In general, the adsorption of a charged species from solution will induce a charge on the metal surface, the magnitude of which will depend on all parameters that affect the electrostatic potential distribution. For the adsorption of a positively charged phospholipid monolayer, the E_{PZC} shifts to a more positive potential. The plot of σ_m vs E, Figure 5, allows a graphical means of determining the shift in E_{PZC} due to adsorption of the lipid layer. The intersection of a horizontal dashed line corresponding to $\sigma_m = 0$ with the σ_m vs E curve defines the E_{PZC} after adsorption, which we will hereafter refer to as E^{ads}_{PZC}. This intersection occurs at 0.167 V vs E_{PZC}. Thus, adsorption of the charged lipid molecules onto the Hg surface results in a 0.167-V shift in the potential of zero charge.[27]

Figure 6 shows the potential distribution across the lipid-coated electrode interface for values of f between 0.000 34 and 0.999 66, calculated using the same set of

(27) A more precise value can be derived from eq 12 by setting $\sigma_m = 0$ to yield $\phi_m^{pzc} = C_2^{-1}\sigma_1 + \phi_2$, where σ_1 is obtained from eq 15 and ϕ_2 is calculated from eq 3c and 3d, under the condition that $\sigma_m = 0$.

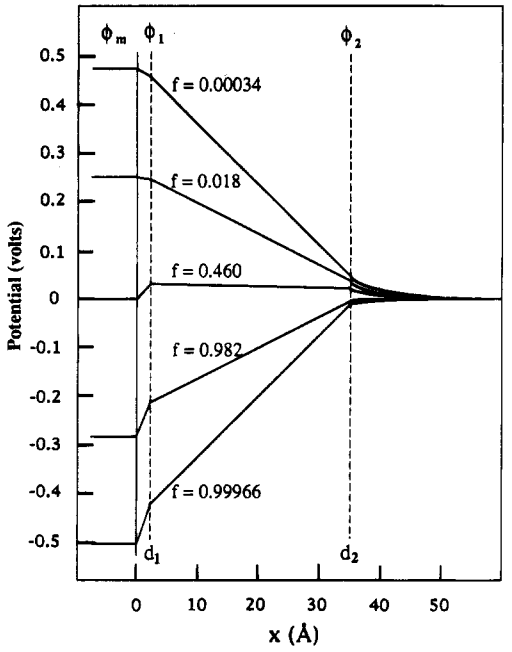

Figure 6. Potential distribution across the Hg/lipid monolayer interface as a function of applied potential, corresponding to the voltammetric response shown in Figure 4.

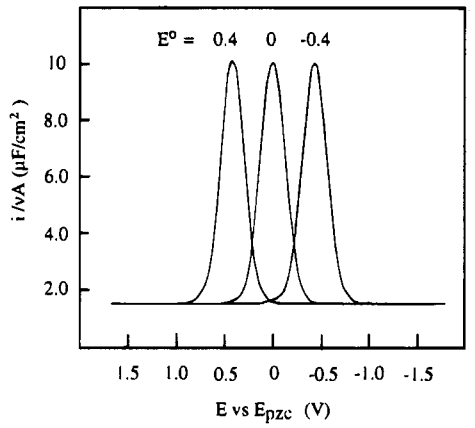

Figure 7. Voltammetric response as a function of $E°$. All other system parameters are the same as in Figure 4.

system parameters employed above. As anticipated from the previous results, most of the potential drop occurs across the region defined by the long hydrocarbon tail of the phospholipid (from d_1 to d_2). Regardless of the applied potential, the potential drop in the solution phase is small for electrolyte concentrations > 0.1 M, a consequence of $C_2 < C_{dif}$ for all values of f. Figure 6 also demonstrates that the E_{PZC} changes upon adsorption of a positively charge molecule. At $E = 0$ (which corresponds to $E = E_{PZC}$ of the bare electrode), the electric field at the surface is seen to have a finite negative value, as evidence by the non-zero positive slope of the potential profile between $x = 0$ and $x = d_1$. Thus, it is immediately apparent that a finite negative charge exists on the electrode surface at this potential. The corresponding shift in the E_{PZC} to E_{PZC}^{ads} that results from this induced charge may be calculated as described in the previous paragraph.

Figures 7–9 show the effects of varying the following parameters: $E°$, Γ_T, C_{elec}, ϵ_1/d_1, and ϵ_2/d_2. Varying $E°$ between ±0.4 V has the effect of shifting the voltammetric wave on the potential axis, Figure 7, by an amount approximately equal to $E°$. The linear dependence of the wave position on $E°$ is a consequence of the fact that virtually all of the interfacial potential drop occurs in the

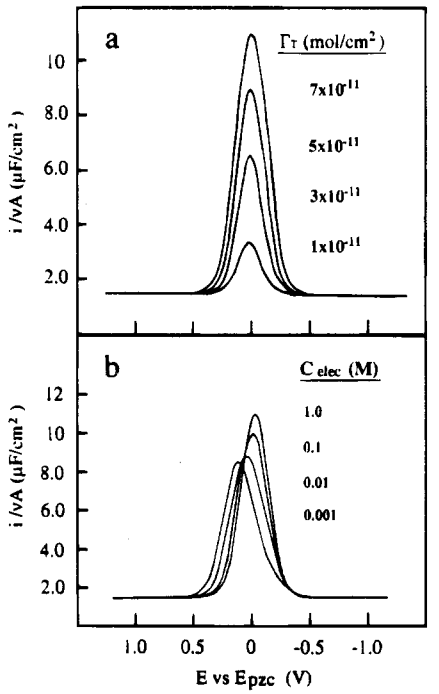

Figure 8. Voltammetric response as a function of (a) surface coverage, Γ_T, and (b) electrolyte concentration, C_{elec}. All other system parameters are the same as in Figure 4.

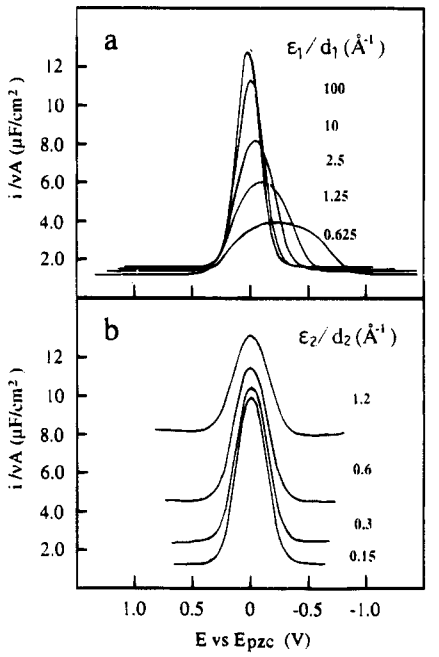

Figure 9. Voltammetric response as a function of (a) ϵ_1/d_1 and (b) ϵ_2/d_2. All other system parameters are the same as in Figure 4.

region between d_1 and d_2, as shown in Figure 6 (i.e., $\phi_1 - \phi_2 \approx E$, neglecting the small potential drops between $x = 0$ and d_1 and in the solution phase). The potential drop, $\phi_1 - \phi_2$, determines the conformation of the monolayer, and eq 8 shows that changing the value of $E°$ has the effect of adding a constant value (=$E°$) to the driving force that is necessary to induce the conformational transition. The key point here is that an experimental measurement of wave position (vs E_{PZC}) allows a direct estimation of the free-energy change associated with the conformational transition. It is noteworthy that the voltammetric peak position is not determined by the sign of the charge associated with the polar headgroup. Thus,

amphiphilic layers containing either negatively or positively charged headgroups may exhibit transitions at potentials negative of E_{PZC}. The primary factor determining the peak potential, E_p, is the difference in the nonelectrostatic energy contributions ($\mu_1^\circ - \mu_2^\circ$) of the two molecular conformations. In addition to the shift in E_p, the shape of the voltammetric wave has a finite but very weak dependence on the value of E° (the difference in the shapes of the three waves in Figure 8 is of the order of the width or the pen used to draw the curves).

An increase in Γ_T results in a proportional increase in the voltammetric peak height, Figure 8a (measured relative to the flat baseline capacitive current), in agreement with the predicted dependence of i on Γ_T indicated by eq 17. Increasing the charge on the lipid molecule, z_{mol}, has a similar effect on the voltammetric response (not shown) as increasing Γ_T. In addition to increasing the peak height, an increase in z_{mol} also tends to cause a small broadening of the wave. However, since the dependencies of the voltammetric response on z_{mol} and Γ_T are so similar, there is no simple means of separating the effects of these two factors.

The effect of varying the supporting electrolyte concentration, C_{elec}, on the voltammetric wave is shown in Figure 8b. Lowering C_{elec} induces a significant positive shift in the voltammetric wave, indicating that the driving force for the conformational transition is slightly larger at more positive potentials. This behavior can be rationalized by noting that a decrease in C_{elec} causes a larger fraction of the total interfacial potential drop to occur across the diffuse double layer. From eq 11, an increase in the diffuse double-layer potential ($\phi_2 - \phi_s$) for any fixed electrode potential ($E = \phi_m - \phi_s$) results in a decrease in $\phi_1 - \phi_2$, thereby increasing the driving force for the lipid molecules to reorient with their headgroups toward the electrode surface (see eq 7 and Figure 6). Thus, there is a positive shift in the position of the voltammetric wave.

As shown in Figure 9, the voltammetric response is a relatively strong function of the molecular parameters ϵ_1/d_1 and ϵ_2/d_2. For example, decreasing ϵ_1/d_1 results in a dramatic decrease in the peak height, a broadening of the wave, and a shift in E_p to negative potentials. The dependence is analogous to that observed upon lowering C_{elec} and is a consequence of the capacitance, C_1 (and, therefore, the potential drop, $\phi_m - \phi_1$), in the region between $x = 0$ and d_1, becoming significantly larger as ϵ_2/d_2 decreases. Figure 9b shows that the primary effect of decreasing ϵ_2/d_2 is to increase the baseline capacitive current defined by eq 18. For sufficiently large values of ϵ_2/d_2, the voltammetric wave becomes noticeably broadened, a result of C_2 becoming comparable to C_1 and C_{dif}.

For redox-active monolayers, the coverage Γ_T(mol/cm^2) of electroactive molecules can be readily obtained from integration of the charge defined by the voltammetric wave.[22] No similar method of analysis exists in the literature for electrochemically-inert monolayers. To investigate the possibility of employing the voltammetric response in determining the surface coverage of DOPC on Hg, we have numerically evaluated the charge under the theoretical voltammetric waves, Q_{app}, as a function of the charge corresponding to the actual coverage employed in the calculation, $Q_f (= z_{mol} F \Gamma_T)$.[28] The results are shown in Table 1, as a function of the assumed values of the molecular parameters ϵ_1/d_1 and ϵ_2/d_2 (other parameters used in the calculation are the same as in Figure 4). As seen in Table 1, the charge measured underneath the voltammetric wave is always smaller than the actual value corresponding to the true surface coverage. However, the numerical examples presented in Table 1 show that Q_{app} is never more than ~25% smaller than Q_f over a wide range of ϵ_1/d_1 and ϵ_2/d_2 combinations. Thus, it is possible to obtain reasonably good estimates of Γ_T from the voltammetric response.

Table 1. Comparison of Apparent (Q_{app}) and True (Q_f) Surface Coverages as a Function of Lipid Monolayer Parameters

	Q_{app},[b] mC/m^2		
Q_f,[a] mC/m^2	$\epsilon_1/d_1 = 0.25$ Å^{-1}, $\epsilon_2/d_2 = 0.14$	$\epsilon_1/d_1 = 0.5$ Å^{-1}, $\epsilon_2/d_2 = 0.14$	$\epsilon_1/d_1 = 2.5$ Å^{-1}, $\epsilon_2/d_2 = 0.5$
12	11	9	7
17	16	13	13
23	21	18	17
29	27	22	22
35	32	27	27
40	38	31	32
46	43	35	36
52	49	40	41
58	54	44	46
64	59	49	50

[a] Q_f = charge corresponding to the true coverage ($z_{mol} F \Gamma_T$). [b] Q_{app} = charge determined from the integrated area under the calculated voltammetric wave (see text and ref 27).

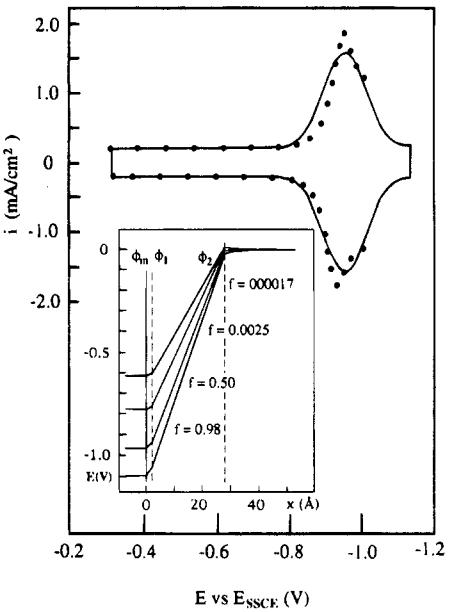

Figure 10. Comparison of experimental voltammogram (solid circles, data from Figure 1) and theoretical response calculated using $E^\circ = -0.475$ V, $E_{PZC} = -0.450$ vs SCE, $\Gamma_T = 2.2 \times 10^{-11}$ mol/cm^2, $z_{mol} = 1$, $C_{elec} = 0.10$ M, $\epsilon_3 = 78$, (a) $\epsilon_1/d_1 = 20$ Å^{-1} and (b) $\epsilon_2/d_2 = 0.241$ Å^{-1}. The inset shows the interfacial potential distribution corresponding to the voltammetric response.

V. Comparison of Experimental and Theoretical Voltammetric Responses of Hg/DOPC. In Figure 10, data from Figure 1 are quantitatively compared to a theoretical voltammogram. Parameters used in computing the theoretical voltammogram were obtained as follows. A value of $\epsilon_2/d_2 = 0.241$ Å^{-1} was computed from the potential-independent capacitive "baseline" current between −0.3 and −0.7 V, using the relationship $i/\nu A = C_T$ and the approximation $C_T \sim C_2$ (as discussed in the preceding section). Next, the peak potential of the

(28) The following equation was employed to calculate Q_{app}: $Q_{app} = [\sigma_m(f_0) - \sigma_m(f_1)] - C_T(f_0)[\phi_m(f_0) - \phi_m(f_1)]$, where $f_0 = 0.000\,01$ and $f_1 = 0.999\,99$ and σ_m, C_T, and ϕ_m are obtained from eqs 9, 14, and 13, respectively. The first term is the total charge on the electrode surface, and the second term is the charge of the surface assuming there is no electroactive film. The capacitance for the second term is assumed as a constant, which is reasonable since the capacitance is dominated by C_2.

experimental voltammogram, $E_p = -0.93$ V, referenced to the E_{PZC} of Hg in a nonadsorbing electrolyte ($E_{PZC} = -0.45$ V vs SSCE in NaF), was used to compute a value of $E°$ for the lipid monolayer from the relationship $E° \approx E_p - E_{PZC}$. The charge on the molecule was taken as +1, and the parameters T, C_{elec}, and z were given their respective experimental values. Finally, the parameters ϵ_1/d_1 and Γ_T were adjusted to yield the best visual fit of the theoretical curves to the data. Values of $\epsilon_1/d_1 = 20$ Å^{-1} and $\Gamma_T = 2.2 \times 10^{-11}$ mol/cm^2 were obtained by this procedure.

The reasonable agreement between the theoretical and experimental voltammograms shown in Figure 10 supports the notion that the peak-shaped voltammogram results from a conformational transition within the lipid monolayer. However, as discussed above, our assumed structures are overly simplified and do not include the possibility of bilayer formation as proposed by Nelson and Leermakers.[13] The fitted value of $\epsilon_2/d_2 = 0.241$ Å^{-1}, corresponds roughly to that expected based on a length of ~16 Å[29] and an effective dielectric constant of ~3.9. This value of ϵ_2 is in reasonable agreement with that expected for the hydrocarbon tail region. On the other hand, the shape of the wave is not particularly sensitive to the chosen value of ϵ_1/d_1, for values of $\epsilon_1/d_1 > 1$, as evident in Figure 9. Thus, our fitted value of $\epsilon_1/d_1 = 20$ Å^{-1} should not be interpreted as a precise value for this parameter. In addition, due to solvation of the charged headgroup and disruption of the solvent structure at the interface,[23b,24b] a precise demarcation of the interface (Figure 3) is somewhat artificial. However, using reasonable values of d_1 (~2 Å) gives a numerical value of $\epsilon_1 = 40$, in agreement with literature values.[30] Given the uncertainty in d_1 and interfacial structure, this value should be interpreted only as a rough estimate of the average permittivity of the headgroup region.

The value of $\Gamma_T = 2.2 \times 10^{-11}$ mol/cm^2 obtained from the fitted data is approximately an order of magnitude smaller than that expected based on molecular models. Our underestimation of Γ_T may indicate that the charge per lipid molecule is considerably less than the assumed value of unity used in the calculation or that only a fraction of the molecules undergo a conformational transition that results in the displacement of charge within the interfacial field. As noted previously, the height (and, thus, the area) of the voltammetric wave has essentially the same dependence on z_{mol} as Γ_T. Thus, a diminution of z_{mol} to 0.1 in the theoretical curve is equivalent to increasing Γ_T by a factor of 10.

The inset in Figure 10 shows the interfacial potential distribution corresponding to the calculated voltammogram. The curves show that the transition between the outward and inward directed conformations does not occur until the potential is significantly negative of the E_{PZC}, a consequence of the relatively greater stability of the monolayer conformation in which the charged headgroups are oriented toward the polar solution phase.

Conclusions

A general analytical method has been developed that allows calculation of the voltammetric response of electrochemically-inert monolayers that are susceptible to field-induced conformational transitions. The model predicts the presence of peak-shaped voltammetric features which are quite consistent with numerous experimental observations. The method provides a means to determine the charge displacement and energetics associated with the conformational transition and can easily be adapted to amphiphilic monolayers with structures and potential-dependent interactions different from those employed in this initial work. However, a rigorous test of this method will require input of potential-dependent structures obtained from direct experimental observations. We are currently carrying out in situ X-ray reflectivity as well as in-plane surface X-ray diffraction studies of these systems which will allow us to make such quantitative comparisons in the future.

Acknowledgment. We gratefully acknowledge support from the Office of Naval Research (X.G., H.S.W., S.C., and H.D.A.) and National Science Foundation (Grant DMR-9107116) (S.C. and H.D.A.).

LA950302S

(29) Wiener, M. C.; White, S. H. *Biophys. J.* **1992**, *61*, 434–447.
(30) Seelig, J.; Macdonald, P. M.; Scherer, P. G. *Biochemistry* **1987**, *26*, 7535–7541.